

THE LARGE-SCALE CLUSTERING OF MASSIVE DARK MATTER HALOES

V. DESJACQUES

*Institute for Theoretical Physics, University of Zürich
Winterthurerstrasse 190, 8057 Zürich, Switzerland*

The statistics of peaks of the initial, Gaussian density field can be used to interpret the abundance and clustering of massive dark matter haloes. I discuss some recent theoretical results related to their clustering and its redshift evolution. Predictions from the peak model are qualitatively consistent with measurements of the linear bias of high mass haloes, which also show some evidence for a dependence on the halo mass M at fixed peak height ν . The peak approach also predicts a distinctive scale-dependence in the bias of haloes across the baryon acoustic feature, a measurement of which would provide strong support for its validity. For 2σ density peaks collapsing at $z = 0.3$, this residual scale-dependent bias is at the 5-10% level and should thus be within reach of very large simulations of structure formation.

1 Peaks in Gaussian random field

The peak model introduced by ¹ assumes that dark matter haloes are associated with peaks of the initial (Gaussian) density field. Although dark matter haloes are the local maxima of the evolved mass distribution, there is a clear correspondence with initial density maxima for massive objects only. In the following, I will focus on the large-scale clustering properties of initial density peaks and show there is nontrivial scale-dependence both in the linear spatial and velocity bias. I will discuss some implications of these results.

2 First order biasing of initial density peaks

Following ¹, one usually smoothes the initial density fluctuations at redshift $z_i \gg 1$ with a filter of characteristic mass scale M before identifying local maxima of height ν . Even though density peaks form a well-behaved point process, the large-scale asymptotics of the 2-point correlation and pairwise velocity can be thought of as arising from the continuous bias relation ^{6,8}

$$\delta n_{\text{pk}}(\mathbf{x}) = b_\nu \delta_M(\mathbf{x}) - b_\zeta \Delta \delta_M(\mathbf{x}), \quad (1)$$

$$\mathbf{v}_{\text{pk}}(\mathbf{x}) = \mathbf{v}_M(\mathbf{x}) - \frac{\sigma_0^2}{\sigma_1^2} \nabla \delta_M(\mathbf{x}), \quad (2)$$

where δn_{pk} and \mathbf{v}_{pk} are the peak count-in-cell density and velocity, δ_M and \mathbf{v}_M are the initial mass density and velocity field smoothed on scale M , and the (Lagrangian) bias parameters b_ν and b_ζ are

$$b_\nu(\nu, \gamma_1) = \frac{1}{\sigma_0} \left(\frac{\nu - \gamma_1 \bar{u}}{1 - \gamma_1^2} \right), \quad b_\zeta(\nu, \gamma_1) = \frac{1}{\sigma_2} \left(\frac{\bar{u} - \gamma_1 \nu}{1 - \gamma_1^2} \right). \quad (3)$$

Here, $\bar{u} \equiv \bar{u}(\nu)$ denotes the mean curvature of peaks of height ν , $\gamma_1(M) = \sigma_1^2/\sigma_0\sigma_2$ and σ_0 , σ_1 and σ_2 are spectral moments which depend upon the shape of the linear mass power spectrum. Note that b_ζ is strictly positive, whereas b_ν can be positive or negative. In Fourier space, wavemodes of the peak number density $\delta n_{\text{pk}}(\mathbf{k})$ can be obtained by multiplying $\delta_M(\mathbf{k})$ with (here and henceforth, I will omit the dependence on ν and γ_1 for brevity)

$$b_{\text{pk}}(k) = b_\nu + b_\zeta k^2 . \quad (4)$$

This defines the spatial peak bias at the first order. In practice, the peak-background split approach, which is based on count-in-cells statistics, can also be used to estimate b_ν ³. In this regards, the linear Lagrangian bias b_ν predicted by the peak model is exactly the same as that returned by the peak-background split argument⁸.

The peak velocity $\mathbf{v}_{\text{pk}}(\mathbf{x})$ as defined in Eq.(2) is consistent with the assumption that initial density peaks move locally with the dark matter. However, the 3-dimensional velocity dispersion of peaks is smaller than that of the mass σ_{-1} , i.e. $\sigma_{\text{vpk}}^2 = \sigma_{-1}^2 (1 - \gamma_0^2)$ with $\gamma_0 = \sigma_0^2/\sigma_{-1}\sigma_1$, because large-scale flows are more likely to be directed towards peaks than to be oriented randomly¹. As shown in⁸, this leads to a k -dependence of the peak velocities as can be seen upon taking the divergence of $\mathbf{v}_{\text{pk}}(\mathbf{x})$ and Fourier transforming it,

$$\theta_{\text{pk}}(\mathbf{k}) = \left(1 - \frac{\sigma_0^2}{\sigma_1^2} k^2\right) W(k, M) \theta(\mathbf{k}) \equiv b_{\text{vel}}(k) \theta_M(\mathbf{k}) , \quad (5)$$

where $\theta \equiv \nabla \cdot \mathbf{v}$ is the mass velocity divergence and $W(k, M)$ is the Fourier transform of the filter. This defines the *statistical* velocity bias $b_{\text{vel}}(k)$. Note that $b_{\text{vel}}(k)$ does not depend on ν and, for the highest peaks, remains scale-dependent even though the spatial bias $b_{\text{pk}}(k)$ has no k -dependence in this limit.

3 Redshift evolution of the peak correlation

Pairwise motions induced by gravitational instabilities will distort the primeval peak correlation. The gravitational evolution of the correlation of initial density peaks can be addressed with the Zel'dovich ansatz¹⁴, assuming they behave like test particles moving with the dark matter. In this first order approximation, the gravitationally-evolved peak correlation $\xi_{\text{pk}}(r, z)$ is the Fourier transform of the peak power spectrum⁹

$$P_{\text{pk}}(k, z) = G^2(k, z) [b_{\text{vel}}(k) + b_{\text{pk}}(k, z)]^2 P_M(k, 0) , \quad (6)$$

where $b_{\text{pk}}(k, z) = D(z_i)/D(z)b_{\text{pk}}(k)$ and the function

$$G^2(k, z) = \left(\frac{D(z)}{D(0)}\right)^2 e^{-\frac{1}{3}k^2\sigma_{\text{vpk}}^2(z)} \quad (7)$$

is a damping term induced by velocity diffusion. It is similar to the propagator $G_\delta(k, z)$ introduced in⁴, although the latter involves the matter velocity dispersion σ_{-1} . The first term in the square bracket reflects the fact that peaks stream towards (or move apart from) each other in high (low) density environments, but this effect is k -dependent owing to the statistical velocity bias. Therefore, the Eulerian and Lagrangian linear bias parameters are related according to

$$b_\nu^{\text{E}}(z) \equiv 1 + \frac{D(z_i)}{D(z)} b_\nu(z_i), \quad b_\zeta^{\text{E}}(z) \equiv \frac{D(z_i)}{D(z)} b_\zeta(z_i) - \frac{\sigma_0^2}{\sigma_1^2} . \quad (8)$$

The first relation is the usual formula for the Eulerian, linear scale-independent bias¹¹. The second relation shows that b_ζ^{E} approaches $-\sigma_0^2/\sigma_1^2$ with time.

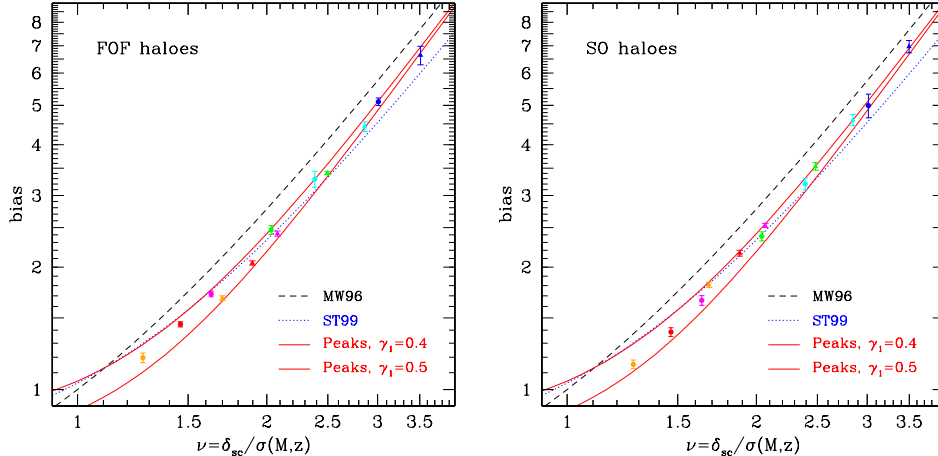


Figure 1: Large-scale bias of dark matter haloes identified with a FOF finder of linking length $b = 0.2$ (left panel) and a SO finder with redshift-dependent overdensity threshold (right panel). Circles and triangles refer to halo samples whose average mass is ~ 1.3 and $5 \times 10^{13} M_{\odot}/h$, respectively. The dotted and dashed curves are formulae based on the excursion set theory, whereas the solid curves are fits motivated by the peak model.

4 The large-scale bias of dark matter haloes

The large-scale bias contains important information on the abundance and clustering of biased tracers of the density field. To compare theoretical expectations with measurements of dark matter halo bias, I will assume that peaks of height $\nu = \delta_c/\sigma_0(R, z)$ identified in the initial, smoothed density field δ_M are associated with objects of mass M collapsing at redshift z .

The peak model predicts that, for moderate peak height, b_{ν}^E is significantly smaller than the value $1 + \nu^2/\delta_c$ derived for thresholded regions¹⁰ due to the correlation between the peak height and the peak curvature¹. However, in the limit $\nu \gg 1$, $b_{\nu}^E(\nu) \approx 1 + (\nu^2 - 3)/\delta_c$ which shows that the evolved linear bias of initial density peaks of height ν indeed converges towards the prediction of¹⁰. This should be compared to well-known expressions derived from the extended Press-Schechter formalism which, in the same limit, evaluate to $b_{\text{MW}}^E(\nu) = 1 + (\nu^2 - 1)/\delta_c$ ¹¹ and $b_{\text{ST}}^E(\nu) \approx 1 + (a\nu^2 - 1)/\delta_c$ ¹². In the latter case, $a = 0.75$ follows from normalising the Sheth-Tormen mass function to N-body simulations. Note that, whereas b_{MW}^E and b_{ST}^E depend only upon the peak height, b_{ν}^E is a function of both ν and M (through $\gamma_1(M)$).

In Fig. 1, these various predictions are compared with measurements of the linear bias of massive haloes extracted from numerical simulations of structure formation⁷. Error bars show the scatter among various realisations. The measured halo bias appears to depart from the Sheth-Tormen scaling at large ν , in agreement with recent measurements of the halo bias^{2,13}. Furthermore, the data shows evidence for a dependence on M , but the exact magnitude of the effect is sensitive to the halo finder. Because the best choice of filter is a matter of debate, I treat γ_1 as a free parameter and show $b_{\nu}^E(\nu, \gamma_1)$ for $\gamma_1 = 0.4$ and 0.5 (a Gaussian filter yields $\gamma_1 \approx 0.65$ for the mass range considered), which provide a reasonably good fit to the bias of $\gtrsim 2\sigma$ haloes. Note that the peak expression b_{ν}^E is also found to match the bias of massive haloes in scale-free cosmologies rather well⁵.

5 Peak biasing and the baryon acoustic oscillation

Having checked that the peak model predicts a large-scale halo bias $b_{\nu}^E(z)$ consistent with simulations, I consider now the impact of the scale-dependent piece $b_{\zeta}^E(z)k^2$. The presence of such a term amplifies the contrast of the baryon acoustic oscillation (BAO) in the correlation of initial

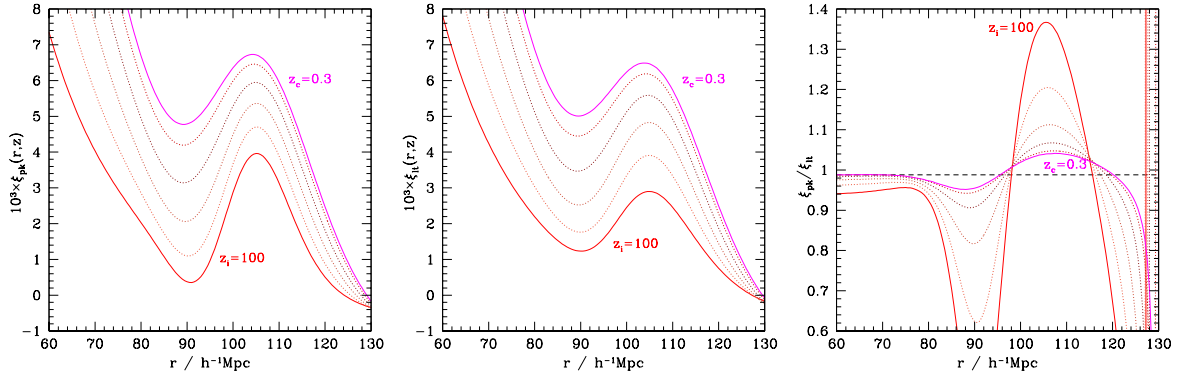


Figure 2: *Left*: Redshift evolution of the baryon acoustic oscillation in the correlation of initial, 2σ density peaks as predicted by Eq.(6). Results are shown at redshift $z = 100, 5, 2, 1.5$ and 0.3 (curves from bottom to top). *Middle*: Same as left panel but for “linear tracers”, for which the correlation simply is $b_V^E(z)^2$ times the evolved mass correlation *Right*: The ratio diverges at $r \sim 130 h^{-1}\text{Mpc}$ because zero-crossings do not coincide

density peaks relative to that in the linear theory correlation⁶. Eq.(6) can be used to estimate how much of this effect survives at virialization redshift (a more realistic calculation should include the mode-coupling power).

To emphasise the effect of $b_V^E(z)k^2$, Fig. 2 compares the redshift evolution of the large-scale, 2-point correlation ξ_{pk} of initial density peaks (left) with that of “linear tracers”, ξ_{lt} , for which $P_{\text{lt}}(k, z) \equiv G_\delta^2(k, z)[b_V^E(z)]^2 P_M(k, 0)$ (middle). The right panel displays the ratio between the two correlations. Results are shown for 2σ density peaks collapsing at $z_c = 0.3$ and identified on a mass scale $5 \times 10^{13} M_\odot/h$ with a Gaussian filter. The relative amplification of the BAO contrast in $\xi_{\text{pk}}(r, z_i)$ induces a scale-dependence in the bias that decays with time owing to the smearing from velocity dispersion. At the collapse redshift however, the model predicts residual scale-dependence across the BAO feature at the 5-10% level (right), a measurement of which in numerical simulations would provide strong support for the validity of the peak approach.

Acknowledgments

I would like to thank the organisers for a very enjoyable meeting.

References

1. J.M. Bardeen, R.J. Bond, N. Kaiser, A.S. Szalay, *Astrophys. J.* **304**, 15 (1986).
2. J.D. Cohn, M. White, *Mon. Not. R. Astron. Soc.* **385**, 2025 (2008)
3. S. Cole, N. Kaiser, *Mon. Not. R. Astron. Soc.* **237**, 1127 (1989).
4. M. Crocce, R. Scoccimarro, *Phys. Rev. D* **73**, 3519 (2006).
5. N. Dalal, M. White, R.J. Bond, A. Shirokov, *Astrophys. J.* **687**, 12 (2008).
6. V. Desjacques, *Phys. Rev. D* **78**, 3503 (2008).
7. V. Desjacques, U. Seljak, I.T. Iliev, *Mon. Not. R. Astron. Soc.* **396**, 85 (2009).
8. V. Desjacques, R.K. Sheth, *Phys. Rev. D* **81**, 3526 (2010).
9. V. Desjacques et al., in preparation (2010).
10. N. Kaiser, *Astrophys. J.* **284**, L9 (1984).
11. H.J. Mo, S.D.M. White, *Mon. Not. R. Astron. Soc.* **282**, 347 (1996).
12. R.K. Sheth, G. Tormen, *Mon. Not. R. Astron. Soc.* **308**, 119 (1999).
13. J.L. Tinker, B.E. Robertson, A.V. Kravtsov, A. Klypin, M.S. Warren, G. Yepes, S. Gottlöber, arXiv:1001.3162
14. Ya.B. Zel’dovich, *Astron. Astrophys.* **5**, 84 (1970)